Structural Engineering and Mechanics, *Vol. 67, No. 5 (2018) 465-479*
DOI: https://doi.org/10.12989/sem.2018.67.5.465

Effective torsional strength of axially restricted RC beams

Cátia S.B. Taborda[1a], Luís F.A. Bernardo*[1] and Jorge M.R. Gama[2b]

[1]*Department of Civil Engineering and Architecture, Centre of Materials and Building Technologies (C-Made), University of Beira Interior, Covilhã, Portugal*
[2]*Department of Mathematics, Center of Mathematics and Applications, University of Beira Interior, Covilhã, Portugal*

(Received August 29, 2017, Revised May 27, 2018, Accepted May 28, 2018)

Abstract. In a previous study, design charts where proposed to help the torsional design of axially restricted reinforced concrete (RC) beams with squared cross section. In this article, new design charts are proposed to cover RC beams with rectangular cross section. The influence of the height to width ratio of the cross section on the behavior of RC beams under torsion is firstly shown by using theoretical and experimental results. Next, the effective torsional strength of a reference RC beam is computed for several values and combinations of the study variables, namely: height to width ratio of the cross section, concrete compressive strength, torsional reinforcement ratio and level of the axial restraint. To compute the torsional strength, the modified Variable Angle Truss Model for axially restricted RC beams is used. Then, an extensive parametric analysis based on multivariable and nonlinear correlation analysis is performed to obtain nonlinear regression equations which allow to build the new design charts. These charts allow to correct the torsional strength in order to consider the favourable influence of the compressive axial stress that arises from the axial restraint.

Keywords: reinforced concrete; beams; torsion; axial restraint; torsional design; charts

1. Introduction

Since the 60s of the last century, several theories have been developed to compute the torsional strength of reinforced concrete (RC) beams. The Space Truss Analogy (STA), which constitutes a simple model to understand the behavior of RC beams under torsion, has deeply influenced a large number of researchers and working groups to set standard rules. As an example, in 1995 the ACI code substituted previous rules based on the skew bending theory by new ones based on the STA. Other codes of practice (e.g., European codes) adopted, right from their origin, rules based on the STA.

The STA assumes that a RC beam under torsion behaves as a thin tube which resists to the external torque with a circulatory shear flow. This tube is analyzed with a space truss analogy, which consists of inclined concrete struts interacting with the longitudinal and transverse reinforcement. This concept is quite enlightening to understand how the compressive concrete and tensile reinforcements resist to the external torque. From the developments of the STA proposed by several authors, one of the most used to characterize the ultimate behavior of RC beams under torsion is the Variable Angle Truss Model (VATM) proposed by Hsu and Mo (1985a). This model aimed to unify small and large cross sections (plain or hollow) and incorporated, for the first time, a smeared stress (σ) - strain (ε) curve for the concrete in compression to account for the softening effect (influence of the diagonal cracking due to transverse tensile stresses) instead of a simple $\sigma-\varepsilon$ curve based on uniaxial tests. By using such a smeared curve the nonlinear behavior of concrete in compression is better incorporated into the models, even for low loading levels (Jeng *et al.* 2011, 2013, Chen *et al.* 2016, Wang *et al.* 2015).

As stated by Bernardo *et al.* (2015a), in structural design of RC members it is common to neglect the influence of the axial restraint due to the connection to other structural members, such as columns and walls. In current situations, RC beams are axially restricted. Hence, among other deformations, the axial deformation is not free. This is mainly true for cracked stage. Therefore, a compressive axial stress state arises, which is generally favorable for the design. For some situations, this favorable effect is considered by codes of practice. Most of the codes provide rules to compute the increase of the shear strength for RC beams due to simultaneous compressive axial states. However, for torsion no rules exist to compute the increase of the torsional strength for similar situations.

This subject is not new and some experimental previous studies exist with RC beams axially restricted in flexure (e.g., Gomes 2011, Lou *et al.* 2011). In such studies it is found that, after cracking, as the axial restraint increases, the stiffness and resistance of the beams increases.

For RC beams axially restricted under torsion, no specific experimental studies were found in the literature. For this reason, Bernardo *et al.* (2015a) proposed the modified VATM for axially restricted RC beams. This

*Corresponding author, Assistant Professor w/ Aggregation
E-mail: lfb@ubi.pt
[a]Assistant Professor
E-mail: tabordacatia@gmail.com
[b]Assistant Professor
E-mail: jgama@ubi.pt

ISSN: 1225-4568 (Print), 1598-6217 (Online)

model was checked with some experimental results with prestress concrete beams under torsion, with external prestress reinforcement. Such technique induces some axial restraint due to the axial stiffness of the prestress bars which are anchored at the ends of the beam. The modified VATM was also checked with some numerical results (Bernardo *et al.* 2015b). From these studies, the authors observed a favorable effect on the torsional strength due to the axial restraint. For this reason, and based on an extensive parametrical analysis, the authors computed and proposed charts to help the design of RC beams under torsion with axial restraint (Bernardo *et al.* 2015a).

In the aforementioned studies, only RC beams with squared cross section were studied. Despite beams with primary torsional moments have cross sections with height to width ratios close to unity, this constitutes a limitation for design. In practical design, rectangular cross sections with height to width ratios higher than unity constitutes a common situation. For this reason, this article presents new torsion design charts, similar to the ones from Bernardo *et al.* (2015a), which cover RC beams with height to width ratios different from unity (rectangular cross sections). For this, extensive parametrical and nonlinear multivariable regression analysis are performed by using the predictions from the modified VATM. The following variable studies are considered: concrete compressive strength, torsional reinforcement ratio, height to width ratio and level of axial restraint. The proposed new charts allow to correct the torsional strength of rectangular RC beams under torsion to account for the favorable influence of the axial restraint. The torsional strength before correction can be computed from current methods, such as from code´s rules.

It should be noted that warping was not considered in this study. In cross-section thin-walled beams, warping is usually an important phenomenon to be considered (Lando 1987, Murín and Kutiš 2008, Chen *et al.* 2016). This study deals with current RC beams with rectangular cross section (plain or hollow). In such members, the torque is mainly resisted through a circulatory flow of tangential stresses (circulatory torsion). However, warping effects can also exist in restrained areas (for instance in the connection areas to other members). In non-cracked stage and in such areas, warping can locally increase the stiffness of the beams. This can affect the torsional capacity of the member (Waldren 1988). However, in the cracked stage and for the ultimate loading, the effects of warping can be highly reduced. This is because the cracks somewhat release the initial restriction and allow the out of plane deformation of the cross section (Waldren 1988). This explains why codes of practice, such as the European codes (Eurocode 2, Model Code 2010), state that for current rectangular RC sections (plain or hollow), the effect of warping can be neglected for the design for the ultimate limit state.

In this article the principal purpose is to study the ultimate behavior of axially restrained RC beams. In this stage the beams are fully cracked. For this reason, the influence of warping was not explicitly considered.

2. The modified VATM for axially restricted beams

To help the reader, this section summarizes the equations and the solution procedure of the modified VATM for axially restricted beams. More details about the assumptions to incorporate the effect of the axial restraint in the VATM, as well as the derivation of the equations, can be found in Bernardo *et al.* (2015a). The methodology to modify the VATM was based from the previous one used by Hsu (1984) to incorporate axial forces in the STA and also by Hsu and Mo (1985b) to incorporate the longitudinal and uniform prestress in the VATM.

In the cracked stage, the length (l) of a RC beam under torsion increases. If no axial restraint exists (free condition), the variation of the beam´s length, Δl, can be simply computed from the average strain in the longitudinal reinforcement, ε_l: $\Delta l = l\varepsilon_l$. If the beam is axially restricted, for instance due to the connection to other structural elements, the stiffness of such elements restrict the axial deformation of the beam. In addition to the torque, a compressive axial stress state arises. The resultant of this stress state, F_c, is directly proportional to the level of axial restraint, k, and to the free elongation of the beam, Δl: $F_c = \Delta l \cdot k$. This resultant force acts on the beam in addition to the torque and must be considered in the equilibrium and compatibility equations of the VATM to derive the modified VATM for axially restricted beams (Bernardo *et al.* 2015a).

As for the VATM, the modified VATM assumes that the external torque is resisted by the equivalent thin tube with a circulatory shear flow, q, which is decomposed into a tensile force acting in the longitudinal reinforcement and a compressive force acting in the concrete struts with an angle α to the longitudinal axis. From Bredt's thin tube theory, the torque T is related to the area enclosed by the center line of the flow of shear stresses (which coincides with the center line of the wall thickness, t_d): $q = T/2A_0$.

The calculation procedure for the modified VATM involves 3 equilibrium equations (see Table 1) to compute the torque, T (Eq. (1)), the effective thickness of the concrete struts of the equivalent hollow section, t_d (Eq. (3)), and the angle of the concrete struts to the longitudinal axis of the beam, α (Eq. (2)). In these equations, σ_d is the stress in the concrete strut, A_l and σ_l are the total area and the stress in the longitudinal reinforcement, respectively, p_0 is the perimeter of the center line of the flow of shear stresses, A_t and σ_t are the area of one bar and the stress in the transverse reinforcement, respectively, and s is the longitudinal spacing of the transverse reinforcement. It should be noted that, despite plain and hollow beams generally behaves differently (Valipour and Foster 2010), for torsion and for the ultimate stage, plain and hollow beams can be considered equivalent since the concrete core can be neglected (Hsu 1984).

To compute the torque (T)-twist (θ) curve from the modified VATM, 3 compatibility equations (see Table 1) are also need to compute the strain in the longitudinal reinforcement, ε_l (Eq. (4)), the strain in the transverse reinforcement, ε_t (Eq. (5)), and the twist, θ (Eq. (6)).

For each input value for the strain at the outer surface of the concrete strut, ε_{ds}, the calculation procedure of the modified VATM starts to compute the strain in the longitudinal reinforcement for the beam without axial restraint. From this value, the elongation of the beam Δl and

Table 1 Equations for the modified VATM

Equilibrium equations		
$T = 2A_0 t_d \sigma_d \sin\alpha\cos\alpha$ (1)	$\cos^2\alpha = \frac{A_l\sigma_l + F_c}{p_0\sigma_d t_d}$ (2)	$t_d = \frac{A_l\sigma_l + F_c}{p_0\sigma_d} + \frac{A_t\sigma_t}{s\sigma_d}$ (3)
Compatibility equations		
$\varepsilon_l = \left(\frac{A_0^2\sigma_d}{p_0 T\cot\alpha} - \frac{1}{2}\right)\varepsilon_{ds,ef}$ (4)	$\varepsilon_t = \left(\frac{A_0^2\sigma_d}{p_0 T\tan\alpha} - \frac{1}{2}\right)\varepsilon_{ds,ef}$ (5)	$\theta = \frac{\varepsilon_{ds,ef}}{2t_d\sin\alpha\cos\alpha}$ (6)
Effective compressive strain in concrete strut		
$\varepsilon_{ds,ef} = \varepsilon_{ds} + \varepsilon_{ds,c}$ (7)	$\varepsilon_{ds,c} = \frac{\varepsilon_{l,c}}{\cos\alpha}$ (8)	$\varepsilon_{l,c} = \frac{F_c}{E_c(A_c - A_h) + A_l(E_s - E_c)}$ (9)

Table 2 $\sigma-\varepsilon$ relationships for materials

Concrete in compression (Belarbi and Hsu 1994, Zhang and Hsu 1998)				
$\varepsilon_{ds} \le \beta_\varepsilon\varepsilon_0$: $\sigma_d = \beta_\sigma f_c'\left[2\left(\frac{\varepsilon_{ds}}{\beta_\varepsilon\varepsilon_0}\right) - \left(\frac{\varepsilon_{ds}}{\beta_\varepsilon\varepsilon_0}\right)^2\right]$ (10a)	$\varepsilon_{ds} > \beta_\varepsilon\varepsilon_0$: $\sigma_d = \beta_\sigma f_c'\left[1 - \left(\frac{\varepsilon_{ds} - \beta_\varepsilon\varepsilon_0}{2\varepsilon_0 - \beta_\varepsilon\varepsilon_0}\right)^2\right]$ (10b)	$\sigma_d = k_1\beta_\sigma f_c'$ (11)		
$\beta_\varepsilon = \beta_\sigma = \frac{R(f_c')}{\sqrt{1 + \frac{400\varepsilon_{c1}}{\eta'}}}$ (12)	$\eta = \frac{\rho_l f_{ly}}{\rho_t f_{ty}}$ (13)	$\begin{cases}\eta' = \eta \text{ if } \eta \le 1\\ \eta' = 1/\eta \text{ if } \eta > 1\end{cases}$ (14)	$R(f_c') = \frac{5.8}{\sqrt{f_c'(\text{MPa})}} \le 0.9$ (15)	
Ordinary reinforcement in tension (Belarbi and Hsu 1994)				
$f_s = \frac{0.975E_s\varepsilon_s}{\left[1 + (1.1E_s\varepsilon_s/f_{sy})^m\right]^{\frac{1}{m}}} + 0.025E_s\varepsilon_s$ (16)	$m = \frac{1}{9B - 0.2} \le 25$ (17)	$B = \frac{1}{\rho}\left(\frac{f_{cr}}{f_{sy}}\right)^{1.5}$ (18)	$f_{cr} = 3.75\sqrt{f_c'(psi)}$ (19)	

the compressive force F_c due to the axial restraint are calculated. With these values, the model calculates the compressive strain of the longitudinal reinforcement $\varepsilon_{l,c}$ due to F_c, which is used to compute the compressive strain of the concrete strut, $\varepsilon_{ds,c}$. This latter is used to compute the effective strain at the outer surface of the concrete strut, $\varepsilon_{ds,ef}$, from which the solution procedure goes on.

Table 1 presents Eq. (7) to (9) to compute the effective strain at the outer surface of the concrete strut, where E_c and E_s are the Young's modulus for concrete and steel bars, respectively, A_c is the area limited by the outer perimeter of the cross section and A_h is the area of the hollow part (for hollow sections).

To characterize the behavior of the materials, smeared and nonlinear $\sigma-\varepsilon$ relationships are used to account for the softening effect (concrete in compression) and stiffening effect (steel bars in tension). As for the softening effect, stiffening effect is also important to be considered here (Khagehhosseini *et al.* 2013, Mondal and Prakash 2015). From several proposals for the $\sigma-\varepsilon$ relationships, Bernardo *et al.* (2012) found that the $\sigma-\varepsilon$ relationship proposed by Belarbi and Hsu (1994) for concrete in compression (Table 2, Eq. (10) and (11)), with the softening coefficient ($\beta_\sigma = \beta_\varepsilon$) proposed by Zhang and Hsu (1998) (Table 2, Eq. (12) to (15)), and the $\sigma-\varepsilon$ relationship proposed by Belarbi and Hsu (1994) for steel bars in tension (Table 2, Eq. (16) to (19)), are suitable to compute the ultimate behavior of RC beams under torsion. These $\sigma-\varepsilon$ relationships were incorporated in the modified VATM.

In Table 2, f'_c is the uniaxial concrete compressive strength, ε_0 is the strain corresponding to f'_c (peak stress), ε_{c1} is the tensile principal strain in the perpendicular direction to the concrete strut, ρ_l and ρ_t are the longitudinal and transverse reinforcement ratios, respectively, f_{ly} and f_{ty} are the yielding stress for the longitudinal and transverse reinforcement, respectively, and f_{cr} is the tensile strength of concrete.

To compute the solution points for the T$-\theta$ curve, a solution procedure based on a trial-and-error technique is used. Fig. 1 presents the flowchart for the solution procedure of the modified VATM. The theoretical failure point of the section is defined from the assumed maximum (conventional) strains for the materials (ε_{cu} for concrete and ε_{su} for steel).

3. Torsion design charts

This section starts to summarize the methodology used by Bernardo *et al.* (2015a) to obtain the design charts for the effective torsional strength of axially restricted RC beams with squared cross section (Section 3.1).

This section also shows the influence of the height to width ratio (h/b) of the cross section on the behavior of RC beams under torsion, in order to justify the need of new torsion design charts to incorporate this new variable study (Section 3.2). To show the influence of h/b, some results obtained from the modified VATM and some experimental

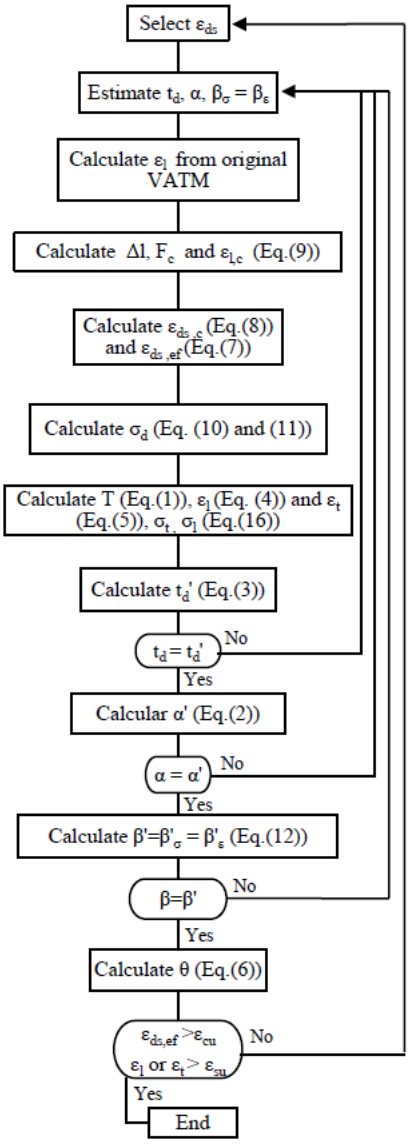

Fig. 1 Flowchart for the calculation of the T–θ curve

results from Hsu (1968) are presented. Finally, the new torsion design charts are presented in Section 3.3.

As in the previous study from Bernardo *et al.* (2015a) and for the other variable studies, the influence of h/b to compute the effective torsional strength of axially restricted RC beams is incorporated through the design charts.

This is because it is not possible to present a simple and practical equation for the influence of such variable and for its correlation with all the other variable studies.

3.1 Torsion design charts for squared RC beams

Bernardo *et al.* (2015a) showed that the influence of the level of axial restraint on the torsional ultimate behavior of RC beams can be relevant. In particular for the torsional strength, the influence of the axial restraint is favorable. For this reason, this effect should be considered in the design of RC beams. To perform an extensive parametric analysis, 3 variable studies (f_c=f'_c, ρ_{tot} and k) with several reference values were considered. From the considered values, 192

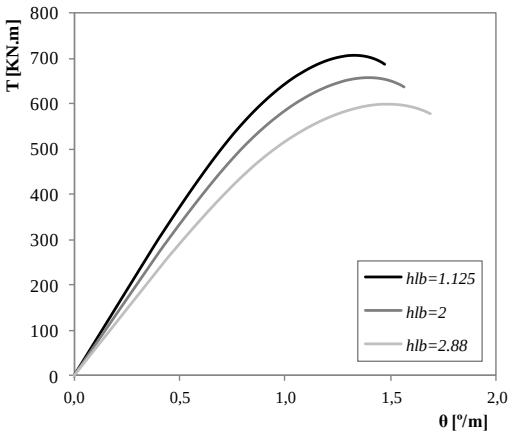

Fig. 2 Theoretical T–θ curves for the idealized RC beams (f'_c=30 MPa, ρ_{tot}=1.0% and A_c=7200 cm^2)

combinations were studied. By using the statistical software "R" with "stats" package to correlate the independent variable studies with the method of least squares, a very accurate polynomial surface of degree 13 (with 171 terms) was found, with a coefficient of determination near to unity, to compute the correction parameter (C_{ca}). From this complex polynomial, design charts were obtained to assist project. Such charts allow to obtain the correction parameter C_{ca} (coefficient of axial confinement) as function of the variables f_c, ρ_{tot} and k, to compute the effective torsional strength ($T_{r,ef}$), from the normal torsional strength (T_r), in order to account for the influence of the axial restraint: $T_{r,ef}$=$C_{ca}T_r$. Details on the methodology to compute parameter C_{ca} and to consider also the influence of the length of the beam, as well as the presentation of the design charts, can be found in Bernardo *et al.* (2015a).

3.2 Influence of the height to width ratio

At this point, it is important to check the influence of the height to width ratio of the cross section, h/b, on the behavior of RC beams under torsion. For this, the modified VATM (with no axial restraint, k=0) is used to compute the behavior of 3 idealized RC beams with equal concrete compressive strength (f'_c=30 MPa), equal torsional reinforcement ratio (ρ_{tot}=ρ_l+ρ_t=1.0%) and equal cross sectional area (A_c=7200 cm^2). In order to variate h/b, while maintaining the other variables fixed, the following cross sections were considered: 80×90 cm (h/b=1.125), 60×120 cm (h/b=2.0) and 50×144 cm (h/b=2.88).

Fig. 2 presents the theoretical T–θ curves for the RC beams. It should be remembered that VATM only provides good results for the ultimate stage (domain to be studied in this study), since it neglects the concrete tensile strength (Hsu and Mo 1985a). For this reason, the transition between the non-cracked and cracked stage is not captured.

The T–θ curves from Fig. 2 show that, as h/b decreases, the torsional stiffness and strength increases, while the ultimate twist decreases. These results show that VATM capture the influence of h/b in the ultimate behavior of RC beams under torsion. This observation justifies new design charts, as the ones previously proposed by Bernardo *et al.*

Table 3 Properties of the test beams from Hsu (1968)

Beam	$x \equiv b$ (cm)	$y \equiv h$ (cm)	$\frac{h}{b}$	x_1 (cm)	y_1 (cm)	f_c' (MPa)	f_{ly} (MPa)	f_{ty} (MPa)	A_l (cm^2)	ρ_l (%)	A_t (cm^2)	s (cm)	ρ_t (%)	ρ_{tot} (%)
B1	25.4	38.1	1.5	21.59	34.29	27.58	313.71	341.29	5.16	0.53	0.71	15.24	0.54	1.07
B2	25.4	38.1	1.5	21.59	34.29	28.61	316.47	319.92	7.92	0.83	1.29	18.09	0.82	1.65
B3	25.4	38.1	1.5	21.59	34.29	28.06	327.50	319.92	11.35	1.17	1.29	12.70	1.17	2.34
B4	25.4	38.1	1.5	21.59	34.29	30.54	319.92	323.36	15.52	1.6	1.29	9.21	1.61	3.21
B5	25.4	38.1	1.5	21.59	34.29	29.03	332.33	321.29	20.39	2.11	1.29	6.99	2.13	4.24
B6	25.4	38.1	1.5	21.59	34.29	28.82	331.64	322.67	25.79	2.67	1.29	5.72	2.61	5.28
G2	25.4	50.8	2.0	21.59	46.99	30.89	322.67	333.71	7.92	0.62	0.71	12.07	0.63	1.25
G3	25.4	50.8	2.0	21.59	46.99	26.82	338.53	327.50	11.35	0.88	1.29	15.56	0.88	1.76
G4	25.4	50.8	2.0	21.59	46.99	28.27	325.43	321.29	15.52	1.2	1.29	11.43	1.2	2.40
G5	25.4	50.8	2.0	21.59	46.99	26.89	330.95	327.50	20.39	1.58	1.29	8.57	1.6	3.18
G6	25.4	50.8	2.0	21.59	46.99	29.92	334.39	349.56	7.74	0.6	0.71	12.70	0.59	1.19
G7	25.4	50.8	2.0	21.59	46.99	30.96	319.23	322.67	11.88	0.93	1.29	14.61	0.94	1.87
G8	25.4	50.8	2.0	21.59	46.99	28.34	321.99	328.88	17.03	1.32	1.29	10.48	1.31	2.63
N1	15.24	30.48	2.0	13.03	28.27	29.51	352.32	341.29	2.85	0.61	0.32	9.21	0.62	1.23
N1a	15.24	30.48	2.0	13.03	28.27	28.69	346.12	344.74	2.85	0.61	0.32	9.21	0.62	1.23
N2	15.24	30.48	2.0	13.03	28.27	30.41	330.95	337.84	5.16	1.11	0.32	5.08	1.13	2.24
N2a	15.24	30.48	2.0	13.03	28.27	28.41	333.02	360.59	5.16	1.11	0.71	11.43	1.1	2.21
N3	15.24	30.48	2.0	13.03	28.27	27.30	351.63	351.63	4.28	0.92	0.32	6.35	0.90	1.82
K1	15.24	49.53	3.25	11.43	45.72	29.85	345.43	354.39	4.28	0.56	0.71	19.05	0.56	1.13
K2	15.24	49.53	3.25	11.43	45.72	30.61	335.77	337.84	7.74	1.03	0.71	10.48	1.03	2.05
K3	15.24	49.53	3.25	11.43	45.72	29.03	315.78	320.61	11.88	1.59	1.29	12.38	1.58	3.17
K4	15.24	49.53	3.25	11.43	45.72	28.61	344.05	339.91	17.03	2.26	1.29	8.57	2.28	4.54
C1	25.4	25.4	1.0	21.59	21.59	27.03	341.29	341.29	2.85	0.44	0.71	21.59	0.44	0.88
C2	25.4	25.4	1.0	21.59	21.59	26.54	334.39	344.74	5.16	0.8	0.71	11.75	0.81	1.61
C3	25.4	25.4	1.0	21.59	21.59	26.89	330.95	329.57	7.92	1.24	1.29	13.97	1.24	2.48
C4	25.4	25.4	1.0	21.59	21.59	27.17	336.46	327.50	11.35	1.76	1.29	9.84	1.76	3.52
C5	25.4	25.4	1.0	21.59	21.59	27.23	328.19	328.88	15.52	2.4	1.29	7.30	2.36	4.76
C6	25.4	25.4	1.0	21.59	21.59	27.58	315.78	327.50	20.27	3.16	1.29	5.40	3.2	6.36

(2015a), to include also the variation of h/b.

To validate the aforementioned results from the modified VATM, a comparative study with some experimental results is performed. For this, the experimental study from Hsu (1968) is considered, in which 28 RC beams of interest for this study were tested under pure torsion. The main properties of such beam are presented in Table 3. Parameters x_1 and y_1 are the width and height of the stirrups, respectively.

Among several performed analysis, the results of the tested beams were used by Hsu (1968) to study the influence of 2 variables which characterize the rectangular cross section: the scale effect (which is related with the area of the cross section) and the height to width ratio of the cross section. Beams from B, G, N, K and C series were used for such study because they allowed to isolate the effect of the previous 2 variables. It should be referred that, from the characteristics of the beams, the effect of each of these 2 variables could not be fully isolated (Hsu 1968).

From the experimental results for beams with balanced reinforcement ($\rho_l=\rho_t$), Hsu (1968) proposed an empirical equation (Eq. (20)) to compute the torsional strength ($T_u=T_r$), as a linear function of parameter Ω. Eq. (20) includes two components for the internal torque: one contributed by the transverse reinforcement ($x_1y_1(A_t/s)f_{ty}$) and another one contributed by the concrete beam without reinforcement (T_0), which can be computed from Saint-Venant's theory.

$$T_u = T_0 + \Omega x_1 y_1 \frac{A_t}{s} f_{ty} \tag{20}$$

In Eq. (20), Ω is the coefficient of proportionality with the internal torque contributed by the transverse reinforcement. In a $x_1y_1(A_t/s)f_{ty}-T_u$ plot, Ω is the slope of the straight line. This parameter is influenced by the dimensions of the cross section (Hsu 1968) and, for this reason, incorporates the influence of h/b.

To evaluate how parameter Ω evolves, Hsu (1968) studied beams from series G and N, with different areas of the cross section and equal h/b. Hsu plotted the graphs $x_1y_1(A_t/s)f_{ty}-T_u$ for these beams and computed the following

Table 4 Comparative analysis for the torsional strength

Beam	$T_{u,exp}$ (kNm)	$T_{u,th}$ (kNm)	$\frac{T_{u,th}}{T_{u,exp}}$
B1	22.26	22.20	0.997
B2	29.26	30.97	1.058
B3	37.51	39.65	1.057
B4	47.34	48.34	1.021
B5	56.15	51.28	0.913
B6	61.69	53.62	0.869
G2	40.34	37.49	0.929
G3	49.60	48.15	0.971
G4	64.85	58.93	0.909
G5	71.97	65.30	0.907
G6	39.09	37.36	0.956
G7	52.65	50.92	0.967
G8	73.44	62.05	0.845
N1	9.10	8.29	0.912
N1a	8.99	8.24	0.916
N2	14.46	12.68	0.877
N2a	13.22	12.42	0.940
N3	12.20	10.95	0.897
K1	15.37	14.63	0.952
K2	23.73	22.47	0.947
K3	28.47	26.82	0.942
K4	35.03	29.86	0.852
C1	11.30	11.04	0.977
C2	15.25	17.59	1.153
C3	20.00	22.68	1.134
C4	25.31	26.02	1.028
C5	29.72	28.34	0.954
C6	34.23	30.23	0.883
		$\bar{x}$ =	0.96
		s =	0.08
		cv =	8.06%

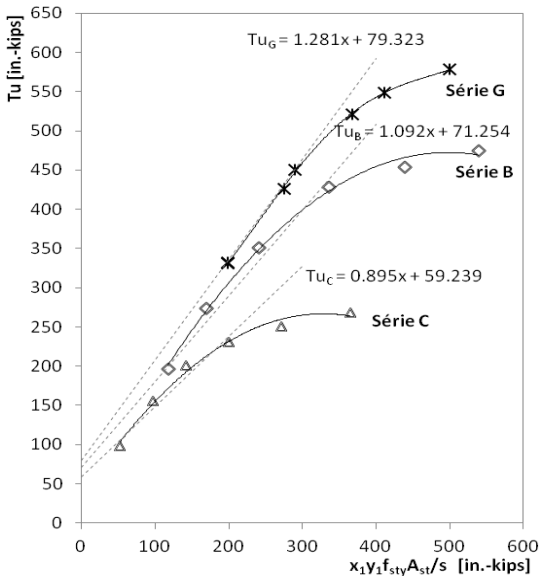

Fig. 3(a) Theoretical results for Ω: Series G, B and C; (1 in-kips = 0.113 kNm)

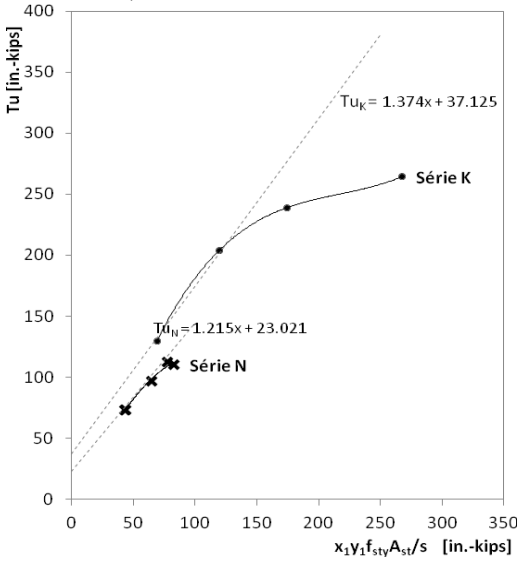

Fig. 3(b) Theoretical results for Series K e N (1 in-kips = 0.113 kNm)

values for parameter Ω: Ω=1.45 for series G and Ω=1.30 for series N. From this result, Hsu concluded that Ω is not constant for beams with different areas of the cross section and with equal *h*/*b*. Hsu also performed a similar analysis for beams with equal width, *b*. For this, Hsu grouped beams from series G, B and C with beams from series N and K, and observed that Ω increases as *h*/*b* increases. However, this analysis do not allow to conclude about the influence of parameter *h*/*b* alone, since this variable was not isolated from the area of the cross section. Hsu fixed the width *b* and the area of the cross section, and correlated the height *h* of the cross section and parameter Ω with y_1/x_1, which is similar to *h*/*b*. Hsu observed that Ω depends on y_1/x_1 and also concluded that the torsional strength also depends on *h*/*b*. From these results, it can be concluded that *h*/*b* influences the behavior of RC beams under torsion.

The aforementioned results confirm the previous theoretical results from the modified VATM (Fig. 2), namely that a real influence of *h*/*b* exists. Therefore, it can be concluded that the modified VATM is valid to study the influence of *h*/*b* on the behavior of rectangular RC beams under torsion.

To confirm the previous statement, the modified VATM is firstly used to compute the theoretical values of the torsional strengths for beams from Table 3. These values are compared with the experimental ones to validate the theoretical model. The results are summarized in Table 4, which presents the experimental ($T_{u,exp}$) and theoretical ($T_{u,th}$) values for the torsional strength, the ratio $T_{u,th}/T_{u,exp}$ and the corresponding values for the mean ($\bar{x}$), standard deviation (*s*) and coefficient of variation (*cv*). From the results, it can be concluded that the modified VATM predicts well the torsional strength of the beams ($\bar{x} = 0.96$) with an acceptable dispersion of the results (*cv*=8.06%).

Table 5 Comparative analysis for the percentage variations of parameter Ω between series

Series	Ω_{Hsu} (%)	$\Omega_{th,VATM}$ (%)
Series C to Series B	26.32	22.01
Series B to Series G	20.83	17.31
Series N to Series K	15.38	13.09

Hence, it can be concluded that the theoretical model can be considered valid to study the ultimate torsional behavior of the RC beams from Table 4.

Next, the modified VATM is used to reproduce the experimental results from Hsu (1968), related with the influence of h/b. in parameter Ω for the RC beams from Table 3. From the theoretical results of Table 4, the theoretical plots $x_1y_1(A_t/s)f_{ty}-T_u$ are presented in Fig. 3(a) and (b), as Hsu (1968) also did with the experimental results (original imperial units were also adopted). Fig. 3 incorporates the theoretical points and the corresponding fitting curves. The straight lines are obtained from a linear regression analysis for the points located in the straight part of the graphs (as Hsu also did). The equation of the straight lines is also given, which allow obtaining the values for the slope (Ω).

From Fig. 3 it can be seen that the modified VATM also capture the variation of parameter Ω, as experimentally observed by Hsu (1968) for the same beams and with the same graphical analysis. Table 5 presents the theoretical and experimental values for the percentage variations of parameter Ω between beams´ series. From Table 5, it can be concluded that the theoretical and experimental trends for the percentage variations of Ω agree, although the theoretical values are slightly underestimated.

From these results, it is confirmed that the modified VATM is valid to study the ultimate behavior of rectangular RC beams under torsion, with different values for h/b and with the other variables fixed.

At this point, it should be referred that, for this study, only values in the range $h/b>1$ are considered. For pure torsion, the geometrical parameter h can always be attributed to the maximum size of the rectangular cross section.

3.3 New torsion design charts

This section aims to present the new design charts for the correction parameter to compute the effective torsional strength of rectangular RC beams axially restricted, considering the influence of variable h/b, in addition to the other variable studies. To obtain these new design charts, new correlations between the increment of the torsional strength, due to the axial restraint, and the variable studies are need, namely with: concrete compressive strength, f_c, torsional reinforcement ratio, ρ_{tot}, level of axial restraint, k, and height to width ratio of the cross section, h/b.

Based on the previous study from Bernardo *et al.* (2015a), the same reference values were adopted for variables f_c, ρ_{tot}, and k. For variable k the following values were considered: 0, 10000, 20000, 30000, 40000, 50000, 60000, 70000 and 80000 kN/m. The range of these values was considered to be representative for the axial restraint of beams in current structures (Bernardo *et al.* 2015a). For variable ρ_{tot} the following values were considered: 0.2, 0.3, 0.4, 0.6, 0.8, 1.0, 1.2, 1.4 and 1.6%. The range of these values include RC beams with brittle and ductile torsional failures and also the minimum ($\rho_{tot,min}$) and maximum ($\rho_{tot,max}$) values from ACI code (Bernardo *et al.* 2015a), which are used as reference values. For variable f_c the following values were considered: 30, 50, 70 and 90 MPa.

The range of value for variable h/b is defined by checking the cross section of several RC test beams under torsion found in the literature (Hsu 1968, Lampert and Thurlimann 1969, Leonhardt and Schelling 1974, McMullen- and Ragan 1978, Rasmussen and Baker 1995, Koutchoukali and Belarbi 2001, Bernardo and Lopes 2009, Fang and Shiau 2004, Chiu *et al.* 2007, Peng and Wong 2011, Jeng 2015). From these test beams, the following values were considered for variable h/b: 1.0, 1.5, 2.0, 2.5 and 3.0. The same reference beam used by Bernardo *et al.* (2015a) for the parametric analysis is also used here (Beams A2 from Bernardo and Lopes 2009). To variate h/b, the width of the cross section was fixed (x=60 cm) and the height variated to obtain the previous values.

Based on the values assumed for the variables to be studied, 1980 combinations were defined. For each combination of values for f_c, ρ_{tot}, k and h/b, the modified VATM was used to compute the effective theoretical torsional strength of the corresponding and modified reference beam A2. The obtained values were compared with the ones without axial restraint and, for each case, the correction parameter C_{ca} was computed. Parameter C_{ca} represents the multiplicative coefficient used to correct the torsional strength in order to consider the increment of resistance due to the axial restraint.

From the values obtained for C_{ca}, for each combination, regression equations are found to relate parameter C_{ca} with the variable studies. For each equation, the maximum absolute residue $m.a.r$ for C_{ca} (difference between the sample values for C_{ca} and the corresponding values predicted by fitted equation) and the corresponding coefficient of determination R^2 (which traduces the quality of the fitted equation) are also computed. The regression equations are presented in Eq. (21) ($m.a.r$ = 0.1007722; R^2 = 0.963) and Eq. (22) ($m.a.r$ = 0.2185; R^2 = 0.989), which allow to compute parameter C_{ca} for $\rho_{tot}\geq1$ and $\rho_{tot}<1$, respectively, as function of f_c, ρ_{tot}, k and h/b. For both equations, $m.a.r.$ is very low and R^2 is close to 1. This means that both equations give accurate values for C_{ca} for the considered ranges of the variable studies.

Despite good results were obtained, it was found that the quality of the regression equations can be improved even more if new equations are found by fixing the value for h/b. Tables 6 and 7 present these new equations for $\rho_{tot}\geq1.0\%$, and $\rho_{tot}<1.0\%$, respectively.

Eqs. (21) to (32) were obtained using the statistical software "R" to correlate the independent variable studies. From the combination of values for C_{ca}, as function of f_c, ρ_{tot}, k and h/b, it was observed that the regression curves obtained from the projection of the hypersurfaces in the 5

$$C_{ca} = 0.952642 - \frac{0.120173}{\left(1-1.40316e^{-\left(1.12172\rho_{tot}-0.673867\rho_{tot}^2+0.0645458\rho_{tot}^3+0.161766\rho_{tot}^4\right)}\right)\left(-12.2377+0.388276ln(k)+0.16606ln(k)^2-0.0097932ln(k)^3\right)}\times$$
$$\times\left(-2.46609+0.150894f_c\right)^{0.514211}\frac{0.120173}{1-0.88823e^{-\left(0.440514h/b-0.0770116h/b^2+0.0376857h/b^3\right)}} \quad \text{for} \quad \rho_{tot}\geq 1.0\% \tag{21}$$

$$C_{ca} = 0.462302 + 2.25088e^{1.28543/(\rho_{tot}+0.498429)}\frac{1}{-106.858-103.886log(k)+18.8547log(k)^2-0.826551log(k)^3}\left(-33.631+1.47299f_c\right)^{0.131536}$$
$$\times\left(-3.88162e^{-0.228285h/b}-3.00102e^{0.183825/h/b}\right) \quad \text{for} \quad \rho_{tot}<1.0\% \tag{22}$$

Table 6 Equations to compute C_{ca} for $\rho_{tot}\geq 1.0\%$ and for fixed values of h/b

$$C_{ca} = 0.9787 - \frac{0.0415\left(0.298449+0.0355445f_c\right)^{0.7647}}{\left(1-1.4288e^{-\left(1.16264\rho_{tot}-0.673099\rho_{tot}^2+0.0126148\rho_{tot}^3+0.20004\rho_{tot}^4\right)}\right)\left(-15.479-0.251734ln(k)+0.358804ln(k)^2-0.0195472ln(k)^3\right)} \tag{23}$$

For $h/b = 1.0$ — $m.a.r. = 0.034346$; $R^2=0.988$

$$C_{ca} = 0.98273 - \frac{0.0299041\left(-1.52039+0.0799697f_c\right)^{0.545607}}{\left(1-1.38074e^{-\left(1.11815\rho_{tot}-0.733517\rho_{tot}^2-0.0060333\rho_{tot}^3+0.225546\rho_{tot}^4\right)}\right)\left(-19.7965-0.247016ln(k)+0.371107ln(k)^2-0.0215925ln(k)^3\right)} \tag{24}$$

For $h/b = 1.5$ — $m.a.r. = 0.013838$; $R^2=0.995$

$$C_{ca} = 0.976846 - \frac{0.0195559\left(-1.83513+0.0714293f_c\right)^{0.505805}}{\left(1-1.36989e^{-\left(1.1181\rho_{tot}-0.762088\rho_{tot}^2-0.0459114\rho_{tot}^3+0.24684\rho_{tot}^4\right)}\right)\left(-9.60449-0.707599ln(k)+0.313926ln(k)^2-0.0159733ln(k)^3\right)} \tag{25}$$

For $h/b = 2.0$ — $m.a.r. = 0.028122$; $R^2=0.982$

$$C_{ca} = 0.97701 - \frac{0.00496612\left(-1.69467+0.0631794f_c\right)^{0.542169}}{\left(1-1.59683e^{-\left(1.11294\rho_{tot}-0.670744\rho_{tot}^2+0.00755209\rho_{tot}^3+0.101452\rho_{tot}^4\right)}\right)\left(-5.93624-0.869168ln(k)+0.264946ln(k)^2-0.0128265ln(k)^3\right)} \tag{26}$$

For $h/b = 2.5$ — $m.a.r. = 0.045409$; $R^2=0.965$

$$C_{ca} = 0.966315 - \frac{0.00316092\left(-3.20606+0.114739f_c\right)^{0.508887}}{\left(1-1.59057e^{-\left(1.09491\rho_{tot}-0.675495\rho_{tot}^2+0.00890655\rho_{tot}^3+0.0881585\rho_{tot}^4\right)}\right)\left(-4.97684-1.23051ln(k)+0.294237ln(k)^2-0.013377ln(k)^3\right)} \tag{27}$$

For $h/b = 3.0$ — $m.a.r. = 0.08055$; $R^2=0.94165$

dimensional space into the coordinate planes are not linear and in general non-linearizable. For this reason, nonlinear regression models based on the method of least squares were used, namely with the algorithm proposed by Levenberg (1944) and improved by Marquardt (1963). This algorithm is available with software "R" with package "nlmrt" (*Functions for Nonlinear Least Squares Solutions*), version 2013-9.25. By using this algorithm, the gradient singularity problem was avoided, which is a common problem when Newton-Raphson Method or Gradient Descent Method are used.

The torsion design charts are obtained by using the equations presented in Tables 6 and 7. Such design charts are presented in Fig. 7. For k<10000 kN/m, the estimate of parameter C_{ca} is done by extending linearly each curve through the origin. In such region of the charts, the curves are represented with dashed lines.

In Fig. 7, it can be observed that the design charts incorporate, as references, the curves corresponding to the minimum ($\rho_{tot,min}$) and maximum ($\rho_{tot,max}$) limit for the reinforcement ratio. Such limits where defined from ACI code (2011) to avoid brittle failures due to insufficient or excessive torsional reinforcement.

From the combination of variables f_c, k and h/b with $\rho_{tot,min}$ and $\rho_{tot,max}$, it is possible do obtain the correlation equations for C_{ca} corresponding to $\rho_{tot,min}$ and $\rho_{tot,max}$. By using again the algorithm of Lavenberg-Marquardt, the correlation curves from the corresponding polynomial hypersurfaces were obtained, both with very low *m.a.r* and with R^2 close to 1. This quality was possible to be obtained because perfect correlation almost exists between f_c and $\rho_{tot,min}$, and also between f_c and $\rho_{tot,max}$. This allows to adjust well the polynomial hypersurfaces with one variable less. This is because $\rho_{tot,min}$ and $\rho_{tot,max}$ are computed from equations which incorporate, in addition to other parameters, the variable f_c. As examples, Eqs. (33) and (34) present, respectively, the equation for $\rho_{tot,min}$ for h/b=1.5 (*m.a.r* = 0.059156) and the equation for $\rho_{tot,max}$ for h/b=2.0 (*m.a.r* = 0.00250435).

In Fig. 7, it can be also observed that no reference curve exists for $\rho_{tot,min}$ when f_c=30 MPa. Some inconsistencies are observed for $\rho_{tot,min}$ for this concrete strength range. These kinds of problems were previously observed in other studies and occurs because the equation of the ACI code to compute de minimum torsional reinforcement is mainly empirical (Ali and White 1999).

Table 7 Equations to compute C_{ca} for ρ_{tot}<1.0% and for fixed values of h/b

$C_{ca} = -0.0357243 + 0.0258478e^{1.14247/(\rho_{tot}+0.598468)} \dfrac{(-11.8332 + 0.557364 f_c)^{0.107926}}{0.168727 + 0.0227843 ln(k) - 0.00656124 ln(k)^2 + 0.00032239 ln(k)^3}$	For h/b = 1.0	(28)
m.a.r. = 0.1415; R^2=0.992		
$C_{ca} = 0.437718 + 0.0129698e^{1.48466/(\rho_{tot}+0.575673)} \dfrac{(-9.69657 + 0.423858 f_c)^{0.129804}}{0.57986 - 0.0531652 ln(k) - 0.00252291 ln(k)^2 + 0.000276711 ln(k)^3}$	For h/b = 1.5	(29)
m.a.r. = 0.12451; R^2=0.994		
$C_{ca} = 0.643315 + 0.00314519e^{1.5025/(\rho_{tot}+0.481364)} \dfrac{(-6.45771 + 0.292705 f_c)^{0.166391}}{0.479473 - 0.0791807 ln(k) + 0.003454711 ln(k)^2 - 0.0000296877 ln(k)^3}$	For h/b = 2.0	(30)
m.a.r. = 0.10137; R^2=0.994		
$C_{ca} = 0.701379 - 0.006369e^{1.81589/(\rho_{tot}+0.546983)} \dfrac{(-0.759646 + 0.025322 f_c)^{0.124223}}{-0.636481 + 0.059625 ln(k) + 0.003026 ln(k)^2 - 0.00032 ln(k)^3}$	For h/b = 2.5	(31)
m.a.r. = 0.076825; R^2=0.997		
$C_{ca} = 0.787309 + 0.000807079e^{2.22929/(\rho_{tot}+0.58352)} \dfrac{(-8.87701 + 0.355111 f_c)^{0.151499}}{0.464014 - 0.0870555 ln(k) + 0.00499758 ln(k)^2 - 0.0000736034 ln(k)^3}$	For h/b = 3.0	(32)
m.a.r. = 0.076305; R^2=0.995		

$$C_{ca} = -0.013133 + 0.504272 f_c + 0.001054 f_c^2 + \left(-0.775132 - 0.421383 f_c + 0.001803 f_c^2\right) log\, k + \left(0.795020 + 0.103360 f_c - 0.000592 f_c^2\right)(log\, k)^2 + \\ + \left(-0.097771 - 0.008151 f_c + 5.617 \times 10^{-5} f_c^2\right)(log\, k)^3 \quad (33)$$

$$C_{ca} = 0{,}556031 + 0{,}048703 f_c - 0{,}00073065 f_c^2 + 4{,}0975 \times 10^{-6} f_c^3 + \left(0{,}339074 - 0{,}0314429 f_c + 0{,}00046767 f_c^2 - 2{,}50606 \times 10^{-6} f_c^3\right) log\, k + \\ + \left(-0{,}0600858 + 0{,}00503194 f_c - 7{,}45686 \times 10^{-5} f_c^2 + 3{,}866468 \times 10^{-7} f_c^3\right)(log\, k)^2 \quad (34)$$

In Fig. 7, the design charts are organized as function of the concrete strength range (f_c) and the height to width ratio of the cross section (h/b). To obtain the increment of the torsional strength for a RC beam with axial restraint, the user must previously know the level of axial restraint (k), the torsional reinforcement ratio (ρ_{tot}), the height to width ratio of the cross section (h/b) and the torsional strength (T_r) of the non-restricted RC beam. This latter can be computed, for instance, from code's rules.

The steps to use the torsion design charts are the following ones:

1. Choose the chart as function of h/b and f_c;
2. From a given k in the horizontal axis, draw a vertical line to intersect the curve corresponding to ρ_{tot};
3. Project the obtained intersection point (Step 2) into the vertical axis to obtain the correction parameter C_{ca};
4. Compute the effective torsional strength ($T_{r,ef}$) from the equation

$$T_{r,ef} = C_{ca} T_r \quad (35)$$

The reference beam used to perform the parametrical analysis (Beams A2 from Bernardo and Lopes 2009), which led to the torsion design charts, has a length (l) equal to 5.90 m. Bernardo *et al.* (2015a) showed that the used methodology to compute the effective torsional strength for axially restricted RC beams depends on the real beam´s length (l_r). To consider this aspect, instead to incorporate a new variable, l_r, and perform new correlations analysis, the influence of the beam´s length can be considered by correcting the level of axial restraint (k). As previously referred in this paper, the compressive axial force due to the axial restraint is function of k and also of the elongation of the beam for the free condition (Δl). This latter is directly proportional to the real length (l_r). Therefore, to introduce the influence of the beam´s length, the corrected level of axial restraint ($k_{l,cor}$) can be computed from Eq. (36). This value is then used to obtain C_{ca} form the design charts.

$$k_{l,cor} = k \times \frac{l_r}{5.90} \quad (36)$$

3.4 Comparison between design charts

In this section, numerical examples are presented to show the differences between the values obtained for parameter C_{ca} by using the design charts for squared cross sections previously proposed by the authors (Bernardo *et al.* 2015a) and the new ones proposed in this study. The objective is to show that the influence of variable h/b is important to be considered to compute the effective resistance torque of axially restricted RC beams.

Let us consider first a RC beam with squared cross section (h/b=1), compressive concrete strength f_c=70 MPa, total torsional reinforcement ratio ρ_{tot}=1.0% (with balanced reinforcements, ρ_l=ρ_t) and axially restricted with k=50000 kN/m. Parameter C_{ca} is obtained using the design chart corresponding to the assumed concrete strength. By using the previously presented steps to use the torsion design charts (Section 3.3), the following value is obtained from the charts proposed by Bernardo *et al.* (2015a): C_{ca}=1.31

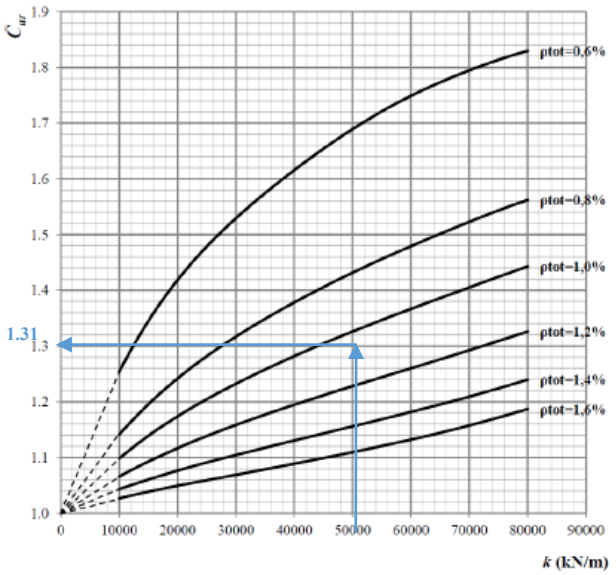

Fig. 4 Example 1: h/b=1, f_c=70 MPa, ρ_{tot}=1.0%, k=50000 kN/m, charts from Bernardo *et al.* (2015a)

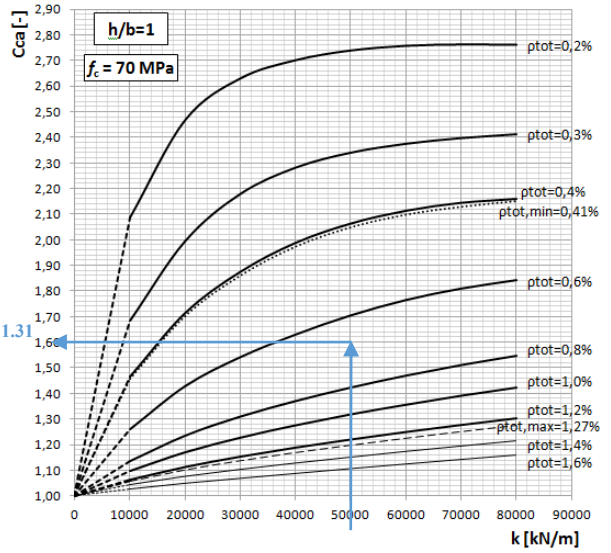

Fig. 5 Example 1: h/b=1, f_c=70 MPa, ρ_{tot}=1.0%, k=50000 kN/m, new charts

(Fig. 4).

For the same previous beam and using the new proposed design charts in this study, the corresponding chart for h/b=1 gives the same value C_{ca}=1.31 (Fig. 5), as expected.

Now let us consider a RC beam with rectangular cross section (h/b=2), compressive concrete strength f_c=70 MPa, total torsional reinforcement ratio ρ_{tot}=1.0% with balanced reinforcements, ρ_l=ρ_t) and axially restricted with k=50000 kN/m. By using the charts proposed by Bernardo *et al.* (2015a), which don't incorporate the influence of h/b, the previous value C_{ca}=1.31 remains valid (Fig. 4). However, by using the corresponding new chart proposed in this study for h/b=2 the following new value is obtained: C_{ca}=1.19 (Fig. 6). As a consequence, the effective resistance torque of the beam is lower by considering the influence of variable h/b.

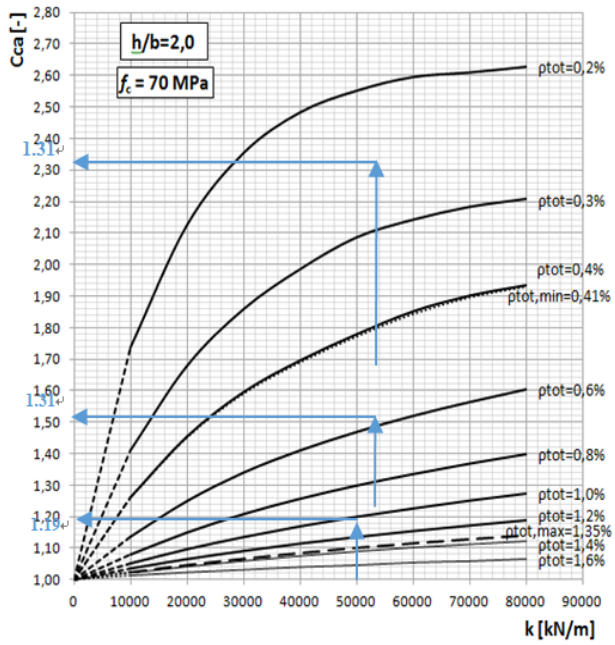

Fig. 6 Example 2: h/b=2, f_c=70 MPa, ρ_{tot}=1.0%, k=50000 kN/m, new charts

4. Conclusions

In this article, new torsion design charts, similar to the charts previously proposed by Bernardo *et al.* (2015a), were proposed to compute the effective torsional strength of rectangular RC beams. For this, in addition to the previous variable studies considered by Bernardo *et al.* (2015a) (f_c, ρ_{tot} and k), the height to width ratio of the cross section was also considered (h/b).

From parametrical and comparative analysis between theoretical results obtained from the modified VATM (Bernardo *et al.* 2015a) and also experimental results from Hsu (1968), the influence of variable h/b on the behavior of RC beams under torsion, namely the torsional strength, was demonstrated. It was observed that the torsional strength decreases as h/b increases. From these analyses, the modified VATM proved to be valid to predict the torsional strength of rectangular RC beams with different values for h/b and with the other variables fixed.

By using the modified VATM and the statistical software "R" with some specific packages, extensive theoretical parametric analysis and multivariable nonlinear correlations were performed to compute the increment of torsional strength due to the axial restraint, as function of the variable studies (f_c, ρ_{tot}, k and h/b) to obtain regression equations.

From the obtained regression equations, new torsion design charts were proposed to compute the effective resistance torque of axially restricted RC beams with rectangular sections. Such charts allow accounting for the favorable influence of the axial restraint in the torsional strength.

Additionally, a simplified procedure was also presented to consider the influence of the real length of the beams to compute the effective torsional strength.

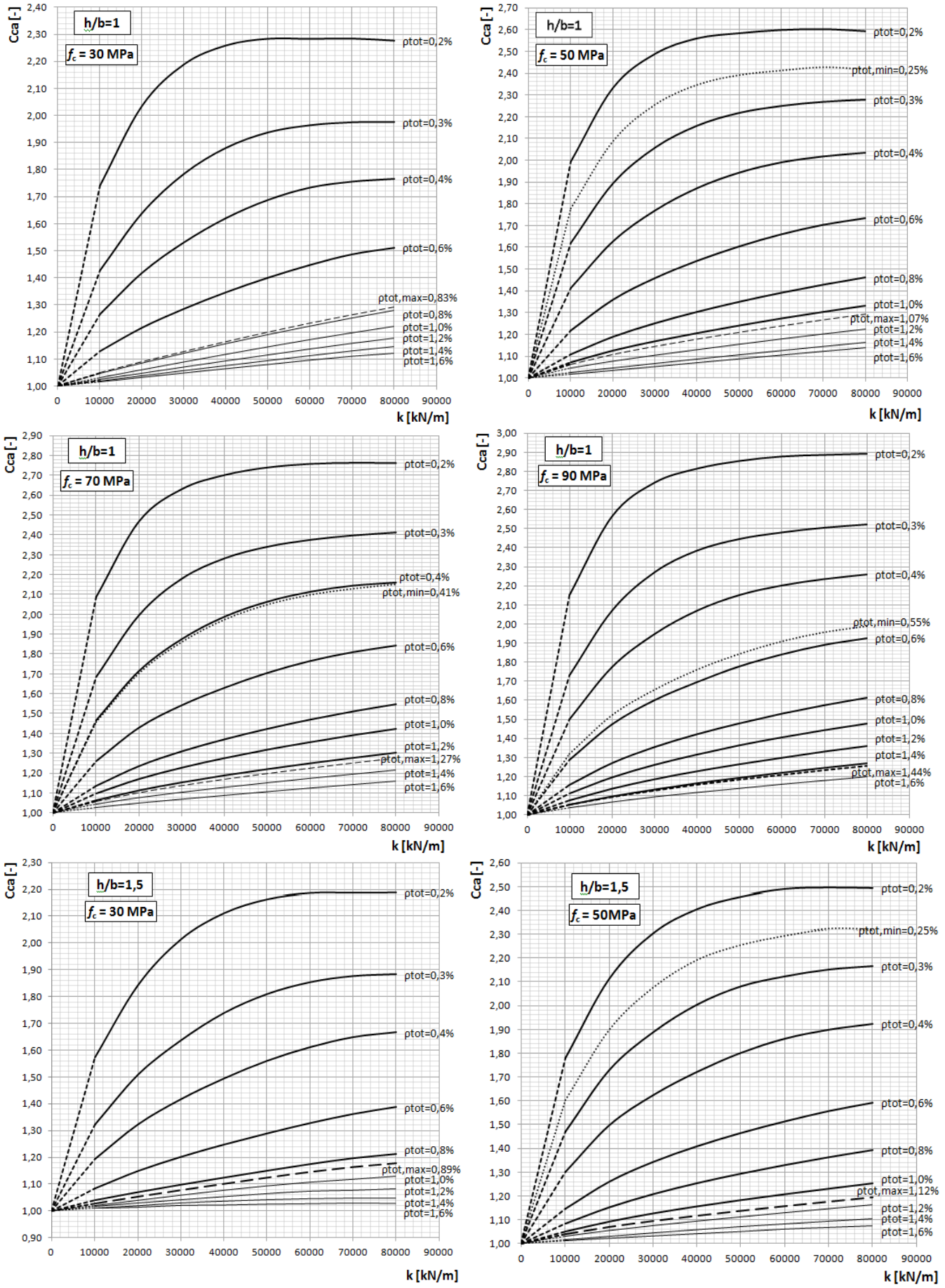

Fig. 7 Torsion design charts

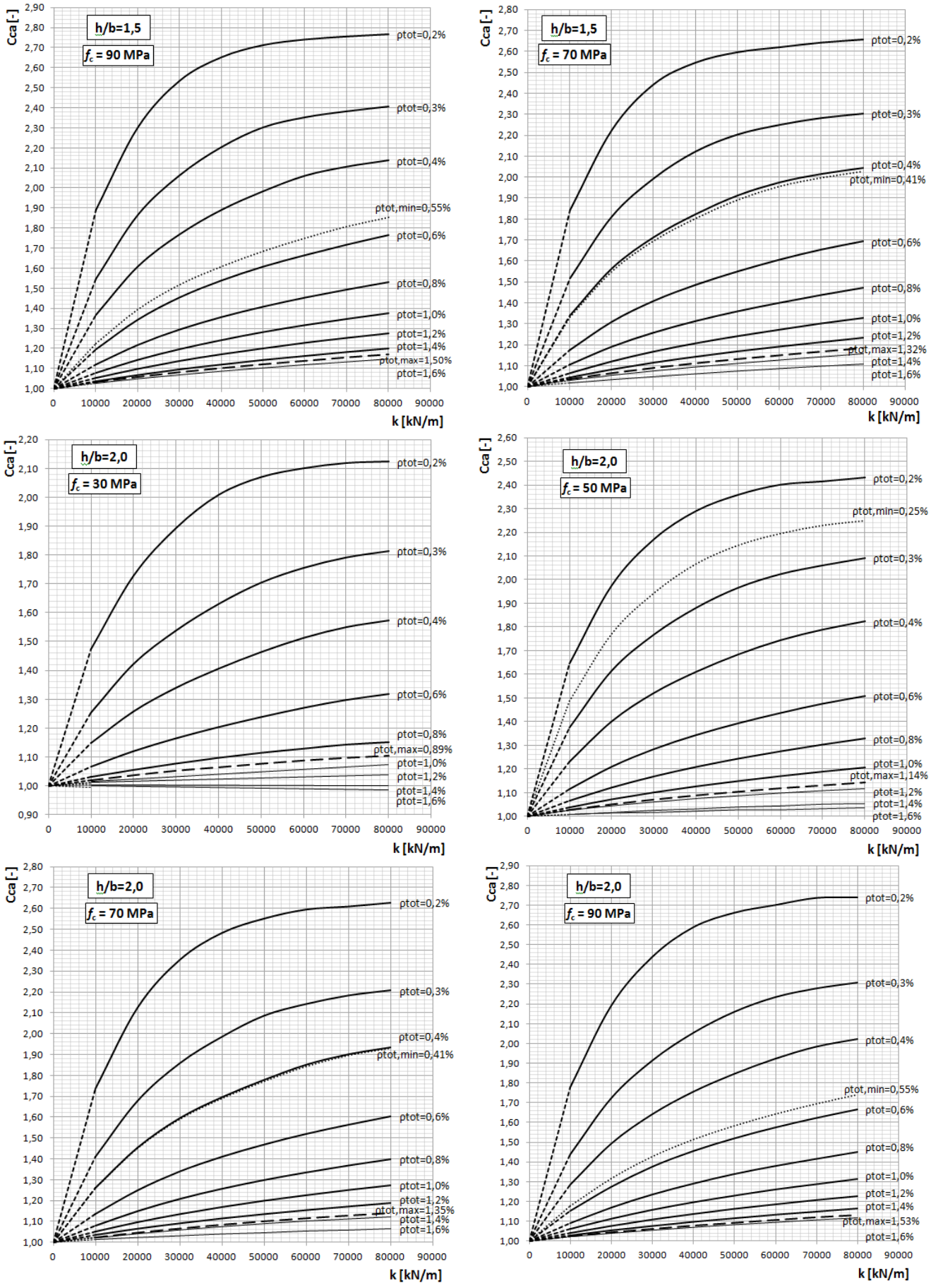

Fig. 7 Continued

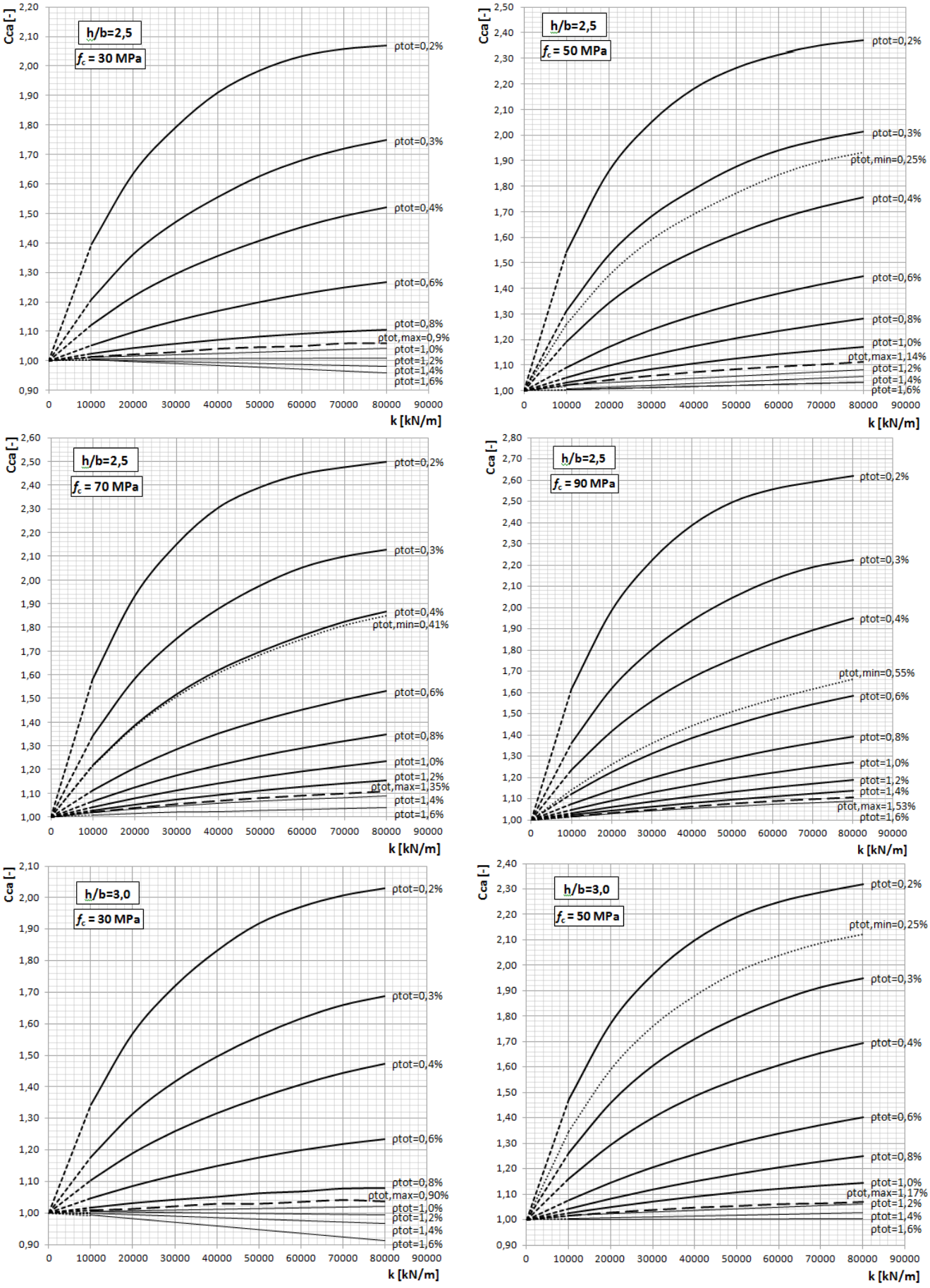

Fig. 7 Continued

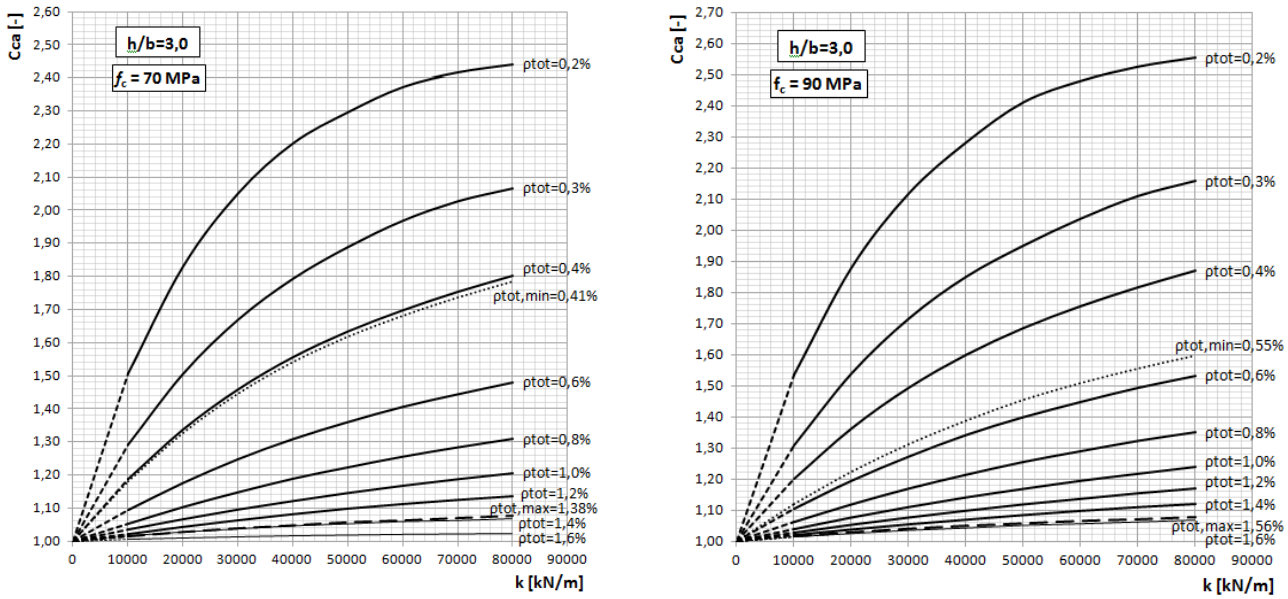

Fig. 7 Continued

References

Ali, M.A. and White, R.N. (1999), "Toward a rational approach for design of minimum torsion reinforcement", *J. Am. Concrete Inst.*, **96**(1), 40-45.

Belarbi, A. and Hsu, T.C. (1994), "Constitutive laws of concrete in tension and reinforcing bars stiffened by concrete", *Struct. J. Am. Concrete Inst.*, **91**(4), 465-474.

Bernardo L.F.A. and Lopes, S.M.R. (2009), "Torsion in HSC hollow beams: Strength and ductility analysis", *ACI Struct. J.*, **106**(1), 39-48.

Bernardo, L.F.A., Andrade, J.M.A. and Lopes, S.M.R. (2012), "Softened truss model for reinforced NSC and HSC beams under torsion: A comparative study", *Eng. Struct.*, **42**, 278-296.

Bernardo, L.F.A., Taborda, C.S.B. and Gama, J.M.R. (2015a), "Parametric analysis and torsion design charts for axially restricted RC beams", *Struct. Eng. Mech.*, **55**(1), 1-27.

Bernardo, L.F.A., Taborda, C.S.B. and Andrade, J.M.A. (2015b), "Ultimate torsional behavior of axially restricted RC beams", *Comput. Concrete*, **16**(1), 67-97.

Chen, S., Ye, Y., Guo, Q., Cheng, S. and Diao, B. (2016), "Nonlinear model to predict the torsional response of U-shaped thin-walled RC members", *Struct. Eng. Mech.*, **60**(6), 1039-1061.

Chiu, H.J., Fang, I.K., Young, W.T. and Shiau J.K. (2007), "Behavior of reinforced concrete beams with minimum torsional reinforcement", *Eng. Struct.*, **29**(9), 2193-2205.

Fang, I.K. and Shiau, J.K. (2004), "Torsional behavior of normal and high-stregth concrete beams", *ACI Struct. J.*, **101**(3), 304-313.

CEB-FIP MODEL CODE (2010), *Comité Euro-International du Béton*, Suisse.

Gomes, D.P. (2011), "Flexural strength of reinforced concrete beams axially restricted", M.Sc. Dissertation, University of Coimbra, Coimbra, Portugal.

Hsu, T.T. (1968), *Torsion of Structural Concrete-Behavior of Reinforced Concrete Rectangular Members*, Torsion of Structural Concrete, SP-18, American Concrete Institute, Detroit, 261-306.

Hsu, T.T.C. (1984), *Torsion of Reinforced Concrete*, Van Nostrand Reinhold Company.

Hsu, T.T.C. and Mo, Y.L. (1985a), "Softening of concrete in torsional members-theory and tests", *J. Am. Concrete Inst.*, **82**(3), 290-303.

Hsu T.T.C. and Mo, Y.L. (1985b), "Softening of concrete in torsional members-prestressed concrete", *J. Am. Concrete Inst.*, **82**(5), 603-615.

Jeng, C.H. (2015), "Unified softened membrane model for torsion in hollow and solid reinforced concrete members-modeling the entire pre- and post-cracking behavior", *J. Struct. Eng.*, **141**(10).

Jeng, C.H., Peng, X. and Wong, Y.L. (2011), "Strain gradient effect in RC elements subjected to torsion", *Mag. Concrete Res.*, **63**(5), 343-356.

Jeng, C.H., Chiu, H.J. and Peng, S.F. (2013), "Design formulas for cracking torque and twist in hollow reinforced concrete members", *ACI Struct. J.*, **110**(3), 457-468.

Koutchoukali, N.E. and Belarbi, A. (2001), "Torsion of high-strength reinforced concrete beams and minimum reinforcement requirement", *ACI Struct. J.*, **98**(4), 462-469.

Khagehhosseini, A.H., Porhosseini, R., Morshed, R. and Eslami, A. (2013), "An experimental and numerical investigation on the effect of longitudinal reinforcements in torsional resistance of RC beams", *Struct. Eng. Mech.*, **47**(2), 247-263.

Lando, M. (1987), "Torsion of closed cross-section thin-walled beams: The influence of shearing strain", *Thin-Wall. Struct.*, **5**(4), 277-305.

Lampert, P. and Thurlimann, B. (1969), *Torsions-Beige-Versuche an Stanhlbetobalken (Torsion Tests of Reinforced Concrete Beams)*, Bericht, No. 6506-2, Institute fur Baustatik, ETH, Zurich, Swiss.

Leonhardt, F. and Schelling, G. (1974), *Torsionsversuche an Stahl Betonbalken*, Bulletin No. 239, Dreurscher Ausschuss Fur Stahlbeton, Berlin, Germany.

Levenberg, K. (1944), "A method for the solution of certain non-linear problems in least squares", *Quarter. Appl. Math.*, **2**, 164-168.

Lou, T., Lopes, A. and Lopes, S. (2011), "Numerical behaviour of axially restricted RC beams", *Proceedings of the International Conference on Recent Advances in Nonlinear Models-Structural Concrete Applications*.

Marquardt, D.W. (1963), "An algorithm for least-squares estimation of nonlinear parameters", *SIAM J. Appl. Math.*, **11**(2), 431-441.

McMullen, A.E. and Rangan, B.V. (1978), "Pure torsion in

rectangular sections: A re-examination", *J. Am. Concrete Inst.*, **75**(10), 511-519.
Mondal, T.G. and Prakash, S.S. (2015), "Effect of tension stiffening on the behaviour of square RC column under torsion", *Struct. Eng. Mech.*, **54**(3), 2131-2134.
Murín, J. and Kutiš, V. (2008), "An effective finite element for torsion of constant cross-sections including warping with secondary torsion moment deformation effect", *Eng. Struct.*, **30**(10), 2716-2723.
Nash, J.C. (1990*), Compact Numerical Methods for Computers. Linear Algebra and Function Minimisation*, 2nd Edition, Adam Hilger, Bristol and New York.
NP EN 1992-1-1 (2010), *Eurocode 2: Design of Concrete Structures-Part 1: General Rules and Rules for Buildings*.
Peng, X.N. and Wong, Y.L. (2011), "Behavior of reinforced concrete walls subjected to monotonic pure torsion-an experimental study", *Eng. Struct.*, **33**(9), 2495-2508.
Rasmussen, L.J. and Baker, G. (1995), "Torsion in reinforced normal and high-strength concrete beams-part 1: Experimental test series", *J. Am. Concrete Inst.*, **92**(1), 56-62.
Valipour, H.R. and Foster, S.J. (2010), "Nonlinear analysis of 3D reinforced concrete frames: Effect of section torsion on the global response", *Struct. Eng. Mech.*, **36**(4), 421-445.
Waldren, P. (1988), "The significance of warping torsion in the design of straight concrete box girder bridges", *Can. J. Civil Eng.*, **15**(5), 879-889.
Wang, Q., Qiu, W. and Zhang, Z. (2015), "Torsion strength of single-box multi-cell concrete box girder subjected to combined action of shear and torsion", *Struct. Eng. Mech.*, **55**(5), 953-964.
Zhang, L.X. and Hsu, T.C. (1998), "Behavior and analysis of 100 MPa concrete membrane elements", *J. Struct. Eng.*, **124**(1), 24-34.

CC